DOI: 10.1002/ejic.201100727

Relaxor Behavior in a New Aurivillius Oxide – $Bi_2La_{0.5}Sr_{0.5}Nb_{1.75}Sc_{0.25}O_9$

Thathan Sivakumar*[a] and Mitsuru Itoh*[a]

Keywords: Aurivillius oxides / Relaxor behavior / Dielectric properties / Perovskite phases / Solid-state structures

A new relaxor type n = 2 Aurivillius oxide material, $Bi_2La_{0.5}Sr_{0.5}Nb_{1.75}Sc_{0.25}O_9$ (**I**), containing heterovalent A and B site cations was synthesized by standard solid-state reaction. The crystal structure of **I** was determined by Rietveld refinement of the powder X-ray diffraction data in the polar $A2_1am$ space group [a = 5.5152(5) Å, b = 5.5199(5) Å, c = 25.1982(12) Å; V = 767.12(10) Å^3] at room temperature. Dielectric measurements for **I** reveal broad dielectric maxima that shift to higher temperature with increasing frequency. The dielectric maximum temperature (T_{max}) at 100 kHz for **I** is 468 K, which is higher than that of the well-known relaxor type Aurivillius oxide $BaBi_2Ta_2O_9$. The relaxation parameter (γ), obtained from a modified Curie–Weiss law for **I**, is 1.91. The piezoelectric coefficient (d_{33}) and remanent polarization (P_r) for the poled sample of **I** are 3 pC/N and 5.7 μC/cm^2, respectively.

Introduction

Relaxor ferroelectrics have been attracting considerable attention owing to their interesting physical properties.[1] Lead-based perovskite relaxor materials such as $PbMg_{1/3}Nb_{2/3}O_3$ (PMN)[1] and PLZT (La-doped $PbZr_{1-x}Ti_xO_3$)[1] have been widely studied. Aurivillius phases[2,3] are layered perovskite oxides of general formula $(Bi_2O_2)(A_{n-1}B_nO_{3n+1})$, where n is the thickness of perovskite slabs. Typical examples are Bi_2WO_6 (n = 1), $Bi_2SrTa_2O_9$ (n = 2), $Bi_4Ti_3O_{12}$ (n = 3). Only few Aurivillius oxide materials are known to exhibit relaxor behavior. The Ba-containing phases, $BaBi_2M_2O_9$ (M = Nb, Ta)[4] show relaxor behavior, and $BaBi_2Ta_2O_9$ (BBT) was found to exhibit good polarization retention up to 10^{12} switching cycles for nonvolatile memory applications. Another set of Aurivillius oxides with heterovalent A-site cations (K^+ and La^{3+}), namely $Bi_2K_{0.5}La_{0.5}Nb_2O_9$[5] and $Bi_2K_{0.5}La_{0.5}Ta_2O_9$,[6] also show relaxor behavior. Recently it has been shown that, when 20% of the Pb in $Bi_2PbNb_2O_9$ ($Bi_2Ba_{0.2}Pb_{0.8}Nb_2O_9$) is replaced by Ba,[7] the resulting material adopts relaxor properties. Relaxor behavior is generally characterized by diffuse phase transitions with strong frequency dependence.[8] Recently, we found that small amounts (2.5–7.5%) of substitution of Sc in the Ta site with compensating trivalent cations $2Bi^{3+}$ and or $2La^{3+}$ in the Sr site in $SrBi_2Ta_2O_9$ (SBT) facilitate the formation of new ferroelectric materials with significantly increased remanent polarization values (two times that of SBT) and/or lower coercive field with relatively defect free materials.[9] Interestingly, for the Nb analogue, we investigated that the piezoelectric constant (d_{33}) for $Bi_{2.5}Sr_{0.5}Nb_{1.75}Sc_{0.25}O_9$[10] is two times as high as that of $SrBi_2Nb_2O_9$ (SBN) with a higher ferroelectric to paraelectric phase-transition temperature (T_c). During our investigations for the design of new relaxor materials containing not only heterovalent A-site cations but also heterovalent B-site cations, we found that $Bi_2La_{0.5}Sr_{0.5}Nb_{1.75}Sc_{0.25}O_9$ exhibits relaxor behavior with relatively higher T_{max}. The details of the synthesis, crystal structure, dielectric, piezoelectric, and ferroelectric properties of $Bi_2La_{0.5}Sr_{0.5}Nb_{1.75}Sc_{0.25}O_9$ are discussed in this communication.

Results and Discussion

The formation of $Bi_2Sr_{0.5}La_{0.5}Nb_{1.75}Sc_{0.25}O_9$ was systematically investigated at various temperatures and times of reaction in air. Powder X-ray diffraction patterns revealed the formation of the target material after 12 h at 1323 K. The crystal structure of $Bi_2Sr_{0.5}La_{0.5}Nb_{1.75}Sc_{0.25}O_9$ was determined by Rietveld refinement of the powder XRD data. Rietveld refinement for $Bi_2Sr_{0.5}La_{0.5}Nb_{1.75}Sc_{0.25}O_9$ was carried out at room temperature with the polar $A2_1am$ and the nonpolar $Amam$ space groups. The coordinates of $SrBi_2Nb_2O_9$[11] and $Ba_{0.375}Pb_{0.625}Bi_2Nb_2O_9$[12] were used as the initial model for the polar $A2_1am$ and the nonpolar $Amam$ space groups, where Sc(12.5%) and La(50%) occupy the Nb(8b) and Sr(4a) sites in $SrBi_2Nb_2O_9$,[11] and Nb(87.5%)/Sc(12.5%) and Sr(50%)/La(50%) occupy Nb(8g) and Ba/Pb(4c) sites in $Ba_{0.375}Pb_{0.625}Bi_2Nb_2O_9$,[12] respectively. $Bi_2Sr_{0.5}La_{0.5}Nb_{1.75}Sc_{0.25}O_9$ crystallizes in the $A2_1am$ space group with a = 5.5152(5) Å, b = 5.5199(5) Å, c = 25.1982(12) Å; V = 767.12(10) Å^3. The refined lattice parameters, a or b and c, are consistent with the ionic radii[13] [the ionic radii for Sr^{2+}(12 CN), Bi^{3+}(8 CN), La^{3+}(12 CN), Nb^{5+} (6 CN), Sc^{3+} (6 CN), and O^{2-} (6 CN) are 1.44,

[a] Materials and Structures Laboratory,
Tokyo Institute of Technology,
4259 Nagatsuta, Yokohama 226-8503, Japan
E-mail: thathansivakumar@gmail.com
sivakumar246810@yahoo.com
itoh.m.aa@m.titech.ac.jp

1.17, 1.36, 0.64, 0.745, and 1.40 Å, respectively]. The observed changes in lattice parameters/cell volume (Table 1) corresponded to the inclusion of the largest d^0 cation, Sc^{3+}, in the B site (increase in *c*/cell volume) with the compensating smaller trivalent cation ($2La^{3+}$) in the A site of the Aurivillius phase. The final Rietveld profile fit is shown in Figure 1. The refined structural parameters are given in Table 1. Selected bond lengths are also listed in Table 1. The structure of $Bi_2Sr_{0.5}La_{0.5}Nb_{1.75}Sc_{0.25}O_9$ consists of perovskite slabs containing $(Nb/Sc)O_6$ octahedra that are interleaved by (Bi_2O_2) layers (see Figure 2). Cation disordering of Sr^{2+} (13%) in Bi_2O_2 layers were also observed in the refinement (see Table 1). Mixing of La^{3+} (4a site) with Bi^{3+} (8b site) yielded larger R_{wp} values (12.18%) for the $A2_1am$ space group, and thus the occupancy of La^{3+} was fixed at the 4a site. Nb/Sc–O bond lengths range from 1.851(23) to 2.198(2) Å.

Table 1. Refined atomic coordinates, isotropic displacement parameters (B_{iso}), and occupancies for $Bi_2La_{0.5}Sr_{0.5}Nb_{1.75}Sc_{0.25}O_9$.[a]

Atom	Wyck.	*x*	*y*	*z*	B_{iso} (Å^2)	Occ.
La1	4a	0.2687(21)	0.7533(18)	0.5	2.1(1)	0.5[b]
Sr1	4a	0.2687(21)	0.7533(18)	0.5	2.1(1)	0.23(1)
Bi1	4a	0.2687(21)	0.7533(18)	0.5	2.1(1)	0.27(1)
Bi2	8b	0.25	0.7386(7)	0.70066(7)	2.5(1)	0.87(1)
Sr2	8b	0.25	0.7386(7)	0.70066(7)	2.5(1)	0.13(1)
Nb	8b	0.2571(24)	0.2502(18)	0.58616(10)	0.2(1)	0.875
Sc	8b	0.2571(24)	0.2502(18)	0.58616(10)	0.2(1)	0.125
O1	4a	0.283(12)	0.229(13)	0.5	0.9(3)	1.0
O2	8b	0.309(9)	0.314(9)	0.6608(10)	0.9(3)	1.0
O3	8b	0.527(10)	0.493(13)	0.2412(11)	0.9(3)	1.0
O4	8b	0.465(10)	0.516(12)	0.5711(11)	0.9(3)	1.0
O5	8b	0.542(11)	0.055(10)	0.5863(10)	0.9(3)	1.0

[a] Space group: $A2_1am$. Lattice parameters: a = 5.5152(5) Å, b = 5.5199(5) Å, c = 25.1982(12) Å; V = 767.12(10) Å^3. Reliability factors: R_{wp} = 11.05%; R_p = 8.43%; R_B = 8.84%; and R_f = 6.96%. Selected bond lengths (in Å): Nb/Sc–O1 2.18(1); Nb/Sc–O2 1.93(3); Nb/Sc–O4 1.90(6); Nb/Sc–O4 2.10(6); Nb/Sc–O5 1.91(6); Nb/Sc–O5 2.06(6). Lattice parameters, reliability factors, and selected bond lengths for the nonpolar *Amam* space group are as follows: a = 5.5155(5) Å, b = 5.5197(5) Å, c = 25.1982(12) Å; V = 767.13(10) Å^3. Reliability factors: R_{wp} = 11.45%; R_p = 8.42%; R_B = 8.27%; and R_f = 7.37%. Selected bond lengths (in Å): Nb/Sc–O1 2.198(2); Nb/Sc–O2 1.851(23); Nb/Sc–O4 1.965(4); Nb/Sc–O4 1.965(4); Nb/Sc–O5 2.005(9); Nb/Sc–O5 2.005(9). [b] The La^{3+} occupancy was fixed; see text.

The variation of dielectric permittivity (ε_r) as a function of temperature at different frequencies ranging from 1 MHz to 5 kHz for $Bi_2La_{0.5}Sr_{0.5}Nb_{1.75}Sc_{0.25}O_9$ (**I**) (see Figure 3) reveals the strong dispersion of dielectric maximum temperature (T_{max}) with increasing frequencies. This behavior is characteristics of relaxor ferroelectrics. The ΔT_{max} obtained from the difference in T_{max} between 1 MHz and 1 kHz for **I** is 65 K. The corresponding ΔT_{max} values for BBT and BBN ($BaBi_2Nb_2O_9$) are 40 K[14] and 110 K,[14] respectively. The maximum value of ε_r at 100 kHz for **I** is 341.

The shift in the T_{max} value for **I** toward lower temperatures is attributed to the addition of trivalent La^{3+}/Sc^{3+} ions in the A/B sites. On the other hand, the T_{max} values (at 100 kHz) for the relaxor Aurivillius oxides BBN[15] and BBT[16] are approximately 460 and 342 K, respectively. At

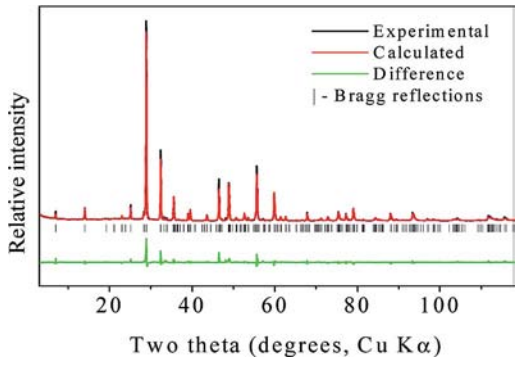

Figure 1. Final Rietveld profile fit for $Bi_2La_{0.5}Sr_{0.5}Nb_{1.75}Sc_{0.25}O_9$ in the $A2_1am$ space group.

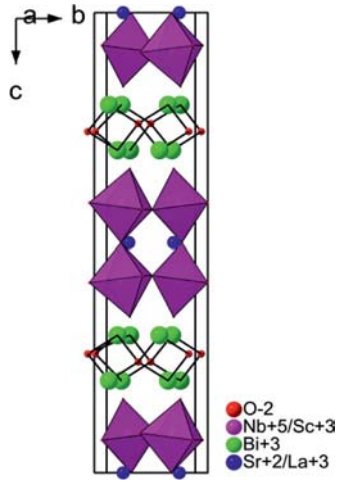

Figure 2. Crystal structure of $Bi_2La_{0.5}Sr_{0.5}Nb_{1.75}Sc_{0.25}O_9$ in the polar $A2_1am$ space group. For clarity, cation disordering was omitted.

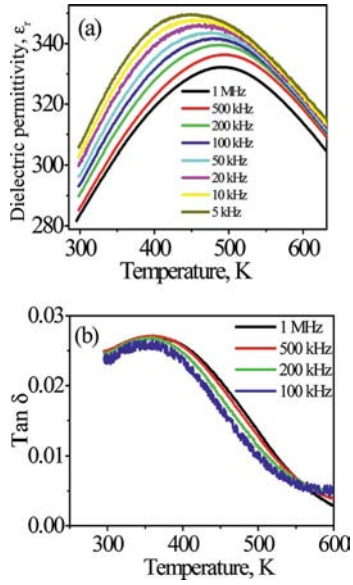

Figure 3. (a) Dielectric permittivity vs. temperature and (b) dielectric loss vs. temperature plots for $Bi_2La_{0.5}Sr_{0.5}Nb_{1.75}Sc_{0.25}O_9$.

100 kHz, the T_{max} for $Bi_2La_{0.5}Sr_{0.5}Nb_{1.75}Sc_{0.25}O_9$ is similar to that for the relaxor Aurivillius oxide containing mono and trivalent A-site cations, $Bi_2K_{0.5}La_{0.5}Nb_2O_9$ (T_{max} = 480 K).[5]

The relaxation behavior is further conformed by the dielectric loss vs. temperature data. For normal ferroelectrics, tanδ decreases with increasing frequency, whereas, for relaxors, tanδ (near the phase-transition temperature) decreases with decreasing frequency, peak temperatures shifting to lower temperatures in a way similar to the dielectric permittivity vs. temperature data. These trends were clearly observed from the dielectric loss vs. temperature plots for **I** (see Figure 3).

The dielectric relaxor behavior is further characterized by the degree of deviation from the Curie–Weiss behavior (ΔT_m) and the relaxation parameter (γ) calculated from the modified Curie–Weiss law. The dielectric constant of a normal ferroelectric is known to follow the Curie–Weiss law, which is described by relation (1).

$$1/\varepsilon_r = (T - T_c)/C \ (T > T_c) \quad (1)$$

In relation (1), T_c is the Curie temperature (i.e., ferroelectric-to-paraelectric phase-transition temperature) and C is the Curie constant.

The Curie–Weiss plot ($1/\varepsilon_r$ vs. temperature), at 100 kHz, for **I** is shown in Figure 4. The Curie constant (C) and T_c for **I** are 2.9×10^5 K and 533 K, respectively. It is observed that for **I**, the T_c obtained from the Curie–Weiss plot is higher than T_{max} (468 K at 100 kHz). Further, the linear fit for the Curie–Weiss plot above T_{max} for **I** reveals that the new compound obeys the Curie–Weiss law above the temperature T_{cw} [T_{cw} could be regarded as the temperature at which the compound deviates from Curie–Weiss behavior, in a linear fit of the $1/\varepsilon_r$ vs. T plot (above the T_m)], which is distinctly higher (T_{cw} = 588 K) (see Figure 4) than T_c. Accordingly, the degree of deviation from the Curie–Weiss behavior could be given by ΔT_m, according to relation (2).

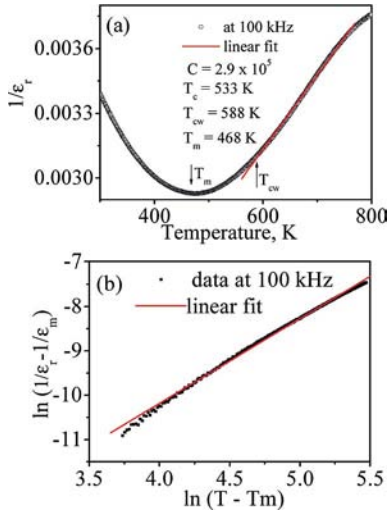

Figure 4. Curie–Weiss (a) and $\ln(1/\varepsilon_r - 1/\varepsilon_m)$ vs. $\ln(T - T_m)$ (b) plots for $Bi_2La_{0.5}Sr_{0.5}Nb_{1.75}Sc_{0.25}O_9$.

$$\Delta T_m = T_{cw} - T_{max} \quad (2)$$

The value of ΔT_m for **I** is 120 K (at 100 kHz). The relaxation parameter (γ) was calculated from the modified Curie–Weiss law, which is given by relation (3).[17]

$$(1/\varepsilon_r) = (1/\varepsilon_m) + (C')^{-1} (T - T_m)^{\gamma} \quad (3)$$

In relation (3), ε_m is the maximum value of the dielectric constant at the transition temperature (T_{max}). C' is the Curie-like constant. The value of γ varies between 1 and 2. For normal ferroelectrics, γ = 1, whereas for an ideal relaxor γ = 2. The γ value obtained from the plot of $\ln(1/\varepsilon_r - 1/\varepsilon_m)$ verses $\ln(T - T_m)$ at 100 kHz (see Figure 4) for **I** is 1.91.

The tolerance factor (t) for the well-known relaxor Aurivillius oxides, namely $BaBi_2M_2O_9$ (M = Nb, Ta)[18] and $Bi_2K_{0.5}La_{0.5}M_2O_9$ (M = Nb, Ta)[5,6] are higher than or equal to 1. The tolerance factor for **I** is much lower than unity (t = 0.964); the substitution of 12.5% of the largest size d^0 cation, Sc^{3+}, in the B site coupled with the smaller A-site cation La^{3+} (the ionic radius of Sr^{2+} is greater than that of La^{3+}) likely attributed to distortion, as evidenced from the a and b lattice parameters (see Table 1), which could lead to crystallization in an orthorhombic system. Rietveld refinements were also performed in the nonpolar orthorhombic *Amam* and the nonpolar tetragonal *I*4/*mmm* space groups. Interestingly, the piezoelectric measurements on **I** revealed that the piezoelectric coefficient (d_{33}) could be defined as the induced polarization in direction 3 [parallel to the direction in which the ceramic element is polarized in direction 3 (3 represents the z-direction)], with a value of 3 pC/N. The low d_{33} value likely results from the cation disordering of Bi^{3+} in (Bi_2O_2 layers) with A-site cations (Sr^{2+} or La^{3+}). In addition, the polarization–electric-field (P–E) measurement for the poled sample of **I** exhibits a P–E hysteresis loop (see Figure 5). The remanent and saturation polarizations for **I** are 5.7 and 8.5 μC/cm^2 at an applied field of 135 kV/cm.

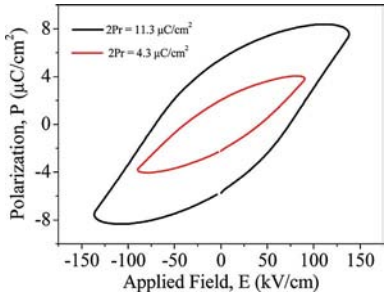

Figure 5. Hysteresis loop (polarization vs. applied electric field) for $Bi_2La_{0.5}Sr_{0.5}Nb_{1.75}Sc_{0.25}O_9$ at two different applied voltages, measured at room temperature.

Conclusions

The positive (non-zero) piezoelectric constant (d_{33}), the ferroelectric behavior, and the crystallographic reliability factors (R values; see Table 1) strongly support the polar $A2_1am$ space group for **I**. From the refined atomic coordi-

nates (see Table 1), we observed a considerable amount of cation disordering, for both the polar $A2_1am$ (13%) and the nonpolar *Amam* (12%) space groups, similar to the nonpolar BBN (13.4%)[11] and BBT[18] in the nonpolar *I*4/*mmm* space group [note that for **I**, refinement in the *I*4/*mmm* space group yielded a larger R_{wp} value (13%)]. Thus, the relaxor behavior in **I**, which could be attributed not only to A-site cation disordering but also to the presence of heterovalent A- and B-site cations, is interesting. We believe that the present work could be extended for the design of new relaxor Aurivillius oxides in general.

Experimental Section

Synthesis: Stoichiometric quantities of Bi_2O_3, $SrCO_3$, Nb_2O_5, and Sc_2O_3 were mixed and heated at 1273 K for 12 h. The resultant powder was ground, formed into pellets, and heated at 1323 K for another 12 h.

Characterization: The products were examined at various stages of the reaction by powder X-ray diffraction (XRD) with a Mac Science MXP18 X-ray diffractometer (Cu-K_α radiation). For structure refinement, the powder X-ray diffraction data were collected in the 2θ range 3–120° with a step size of 0.02° and a step time of 6 s. For dielectric and ferroelectric/piezoelectric measurements, the sintered pellets were polished to a thickness of about 0.5 and 0.3 mm, respectively, and coated with Au electrodes. Dielectric measurements were performed at a field of 1 V/mm with a Hewlett–Packard precision LCR meter (HP4284A) in the temperature range 300–800 K with variable frequencies in the range from 1 MHz to 50 Hz. For ferroelectric and piezoelectric measurements, the sample was poled at 453 K, immersed in silicone oil, kept at an applied field of 100 kV/cm for 0.5 h, and then field-cooled to room temperature. *P*–*E* loops were measured with the ferroelectric measurement system of an aixACT TF Analyzer 2000 with a high voltage amplifier of 10 kV. To prevent possible air breakdown at high field, the sample was immersed in silicone oil during measurements. Piezoelectric coefficients (d_{33}) were measured at room temperature with a Piezo d33 meter (Institute of Acoustics, Chinese Academy of Sciences, ZJ-3B).

Acknowledgments

This work was financially supported by Kakenhi (Nos. 21009087 and 23246113). T. Sivakumar thanks the Japan Society for the Promotion of Science (JSPS) for the award of a postdoctoral fellowship (ID No. P09087).

[1] Y. Xu, *Ferroelectric Materilas and Their Applications*, Elsevier, Amsterdam, **1991**, pp. 101–210.
[2] B. Aurivillius, *Ark. Kemi* **1949**, *1*, 463–480.
[3] B. Aurivillius, *Ark. Kemi* **1950**, *2*, 519–527.
[4] C. A. Paz de Araujo, J. D. Cuchiaro, L. D. McMillan, M. C. Scott, J. F. Scott, *Nature* **1995**, *374*, 627–629.
[5] C. Karthik, N. Ravishankar, K. B. R. Verma, M. Maglione, R. Vondermuhll, J. Etourneau, *Appl. Phys. Lett.* **2006**, *89*, 042905 (3 pp.).
[6] C. Karthik, N. Ravishankar, M. Maglione, R. Vondermuhll, J. Etourneau, K. B. R. Verma, *Solid State Commun.* **2006**, *139*, 268–272.
[7] H. Du, Y. Li, H. Li, X. Shi, C. Liu, *Solid State Commun.* **2008**, *148*, 357–360.
[8] L. E. Cross, *Ferroelectrics* **1994**, *151*, 305–320.
[9] T. Sivakumar, M. Itoh, *Chem. Mater.* **2011**, *23*, 129–131.
[10] T. Sivakumar, M. Itoh, *J. Mater. Chem.* **2011**, *21*, 10865–10870.
[11] S. M. Blake, M. J. Falconer, M. McCreedy, P. Lightfoot, *J. Mater. Chem.* **1997**, *7*, 1609–1613.
[12] R. Macqart, B. J. Kennedy, T. Kamiyama, F. Izumi, *J. Phys. Condens. Matter* **2004**, *16*, 5443–5452.
[13] R. D. Shannon, *Acta Crystallogr., Sect. A* **1976**, *32*, 751–767.
[14] V. V. Shvartsman, M. E. V. Costa, M. Avdeev, A. L. Kholkin, *Ferroelectrics* **2003**, *296*, 187–197.
[15] A. L. Kholkin, M. Avdeev, M. E. V. Costa, J. L. Baptista, S. N. Dorogovtsev, *Appl. Phys. Lett.* **2001**, *79*, 662–664.
[16] P. Keburis, J. Banys, J. Grigas, Z. Bortkevic, A. Kholkin, M. E. V. Costa, *Ferroelectrics* **2007**, *347*, 50–54.
[17] K. Uchino, S. Nomura, *Ferroelectrics* **1982**, *44*, 55–56.
[18] Y. Shimakawa, Y. Kubo, Y. Nakagawa, S. Goto, T. Kamiyama, H. Asano, F. Izumi, *Phys. Rev. B* **2000**, *61*, 6559–6564.

Received: July 14, 2011
Published Online: November 3, 2011

